Phys. Status Solidi C 9, No. 2, 286–289 (2012) / DOI 10.1002/pssc.201100243

physica status solidi c
www.pss-c.com
current topics in solid state physics

Modelling of passive mode-locking in InAs quantum-dot lasers with tapered gain section

Mattia Rossetti*, Tianhong Xu, Paolo Bardella, and Ivo Montrosset**

Dipartimento di Elettronica, Politecnico di Torino, C. so Duca degli Abruzzi 24, 10129 Torino, Italy

Received 20 June 2011, revised 1 August 2011, accepted 8 August 2011
Published online 7 November 2011

Keywords quantum dots, passive mode-locking, tapered lasers, modelling

* Corresponding author: e-mail mattia.rossetti@polito.it, Phone: +39 011 090 4208, Fax: +39 011 090 4217
** e-mail ivo.montrosset@polito.it, Phone: +39 011 090 4159, Fax: +39 011 090 4217

We propose a computationally efficient approach for the simulation and design of index-guided quantum-dot (QD) passively mode-locked lasers with tapered gain section; the method is based on the combination of simulations based on a finite difference beam-propagation-method and dynamic simulations of mode-locking via a multi-section delayed differential equation model. The impact of varying the taper full angle on the pulse duration and peak power is investigated; simulations show that a correct choice of this parameter enables the generation of sub-picosecond optical pulses with peak power exceeding 5 W.

1 Introduction

In the last years, the possibility to generate high power ultra-short optical pulses at 1.3 μm from passively mode-locked lasers with active region consisting of stacked layers of InAs quantum dots (QDs) has been demonstrated [1-3]. In particular significant improvements in terms of pulse width and peak power of the generated pulses have been achieved by considering QD mode-locked lasers with tapered gain sections [1-3]. Modelling and design of such devices is however critical; in principle, distributed time-domain models resolving the field dynamics in both the longitudinal and lateral directions of the laser cavity should be developed [4]; such models have however an extremely high computational cost and, to our knowledge, have never been applied to the simulation of passive mode-locking (ML) in tapered devices where processes with time-scales ranging from sub-picoseconds up to several tens of nanoseconds are involved. In order to overcome this problem, we propose a simplified but computational efficient method for the simulation and design of QD mode-locked lasers (MLLs) with tapered gain sections that involves the use of the multi-section delayed differential equation (MS-DDE) model proposed in [5] where parameters describing the propagation along the non-uniform waveguide are extracted from preliminary simulations using a static finite-difference beam-propagation method (BPM). Despite the approximations introduced, the proposed approach describes the influence of a tapered gain section on the achieved ML regimes. The paper is organized as follows: in Section 2, the MS-DDE model for dynamic ML simulations is briefly described, in Section 3 the BPM simulations allowing to investigate the field transformation across the tapered section and to extract the propagation parameters to be used in the MS-DDE model are shown; the approach is then applied to the analysis of tapered MLLs and the impact of varying the taper angle on the obtained pulse width, peak power and ML stability range is investigated in detail. Finally, a brief conclusion is drawn.

2 Multi-section DDE model

Despite the assumptions and approximations introduced, DDE models represent a powerful and computationally efficient approach for the simulation of ML in semiconductor lasers [6,7]. In [5], we proposed a new MS-DDE model and we demonstrated its effectiveness in providing an improved description of QD MLLs with two-section Fabry-Perot cavity. In addition the MS-DDE model can be successfully applied in the simulation of MLLs with non-uniform waveguides as described in this work.

The model assumes unidirectional lasing in an equivalent ring cavity realized by an arbitrary number of sections, F, that can be either forward biased (gain (G) sections) or

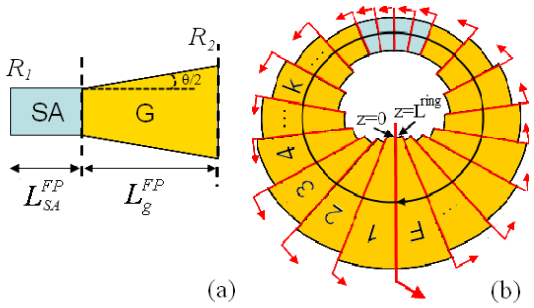

Figure 1 (a) Schematic of a QD ML laser with tapered gain section (G) and reverse-biased saturable absorber (SA); (b) equivalent ring laser; red arrows represent non-saturable losses introduced between any of the two adjacent sections.

reverse-biased (saturable absorber (SA) sections).

Each section is characterized by an arbitrary length, L_k, ridge width, W_k, and field confinement factor, Γ^k_{xy} (describing the overlap between the transverse field profile and the QD active layers under the ridge), being k=1…F. In addition non saturable losses are introduced between any two adjacent sections including both internal losses α_k^{int} (due to propagation in the k^{th} section) and output coupling losses K_k. With respect to standard DDE models [6,7], the above assumptions allow defining a ring laser structure shown in Fig. 1b whose dynamic behaviour is equivalent to the tapered FP MLL shown in Fig. 1a. Referring to Fig. 1, we therefore set $L_g^{Ring}=2\cdot L_g^{FP}$ and $L_{SA}^{Ring}=2\cdot L_{SA}^{FP}$,being L_g^{Ring} and L_{SA}^{Ring} the total length of the gain and SA sections of the ring structure ($L_g^{Ring}+L_{SA}^{Ring}=\Sigma_k L_k$) and L_g^{FP} and L_{SA}^{FP} the corresponding lengths for the FP laser; furthermore, being R_1 and R_2 the reflectivities at the device facet of the FP laser, we set $K_{F/2} = R_1$, $K_F = R_2$ and $K_k = 1$ elsewhere [5].

In the ring laser structure, the dynamics of the slowly varying field amplitude in z =0 (Fig. 1b) at the wavelength resonant with the QD ground state (GS) transitions, $E_{GS}(\tau)$, is then described by the following DDE:

$$\frac{dE_{GS}}{d\tau}(\tau) = -\gamma E_{GS}(\tau) + \gamma R_{GS}(\tau - T)E_{GS}(\tau - T) \qquad (1)$$

where T is the cold cavity round trip time and $R_{GS}(\tau)$ represents the amplification and phase changes experienced by the field during a single round trip in the cavity; $R_{GS}(\tau)$ can be written as:

$$R_{GS}(\tau) = \prod_{k=1}^{F} \exp\left(\frac{1}{2}\Gamma^k_{xy} g_{GS,k}(\tau) L_k\right) \times \exp\left(j\frac{\alpha_{GE}}{2}\Gamma^k_{xy} g_{ES,k}(\tau) L_k\right)\sqrt{K_k}\, e^{-\alpha_k^{int}/2L_k} \qquad (2)$$

where $g_{i,k}(\tau)$, with i = GS, ES, is the gain/absorption induced by the QD GS or first excited state (ES) in the k^{th} section. $\alpha_{GE}/2\cdot\Gamma^k_{xy}g_{ES,k}(\tau)$ represents instantaneous changes in the real part of the propagation constant, induced by the QD ES at the GS wavelength and responsible for a non-zero chirp of the ML pulses due to self-phase modulation [8]; α_{GE} is therefore a coefficient, modelling the strength of this effect [5]. The gain/absorption $g_{i,k}(\tau)$ can be calculated as $g_{i,k}(\tau)=g_{0i}(2\rho_{i,k}-1)$ where $\rho_{i,k}$ is the occupation probability in the i^{th} QD state in the k^{th} section and g_{0i} is the material gain coefficient for i = GS, ES.

The temporal dynamics of $\rho_{i,k}$ in each section is computed by a dedicated system of rate equations describing intraband carrier dynamics in the QD confined states in the quantum well and barrier states in both forward and reverse-biased sections, coupled with (1) via the stimulated emission rate. A detailed description of the considered rate equation systems can be found in [9] and explicit expression for the stimulated emission rate are reported in [5].

In this work, lasers with active region consisting of 10 InAs dot-in-a-well layers will be considered. Material parameters used in the rate-equations can be found in [9].

The numerical solution of the DDE (1) coupled with the system of rate equations governing the dynamics of $g_{i,k}(\tau)$ allows compute the ML regimes as a function of bias and structural parameters in tapered QD MLLs, with simulation time up to twenty times faster than the Finite Difference Travelling Wave model described in [5]. The non-uniform waveguide cross-section is included in the simulations by introducing sections with different values for W_k, Γ^k_{xy} and α_k^{int} where the last two parameters are extracted from preliminary BPM simulations as described in the following section.

3 BPM simulations

We consider tapered QD MLLs with total length $L_{SA}^{FP}+L_g^{FP}$=3 mm, SA length L_{SA}^{FP} = 450 μm, facet reflectivities R_1=0.99 and R_2 = 0.1, and different full angles θ = 0.3°, 0.6°, 1°, 1.5° characterizing the tapered section. A straight QD MML (θ=0°) with the same cavity lengths is also considered as a reference.

In order to extract Γ^k_{xy} and α_k^{int} for each section composing the equivalent ring laser structure (Fig. 1b), a finite-difference BPM (e.g. [10]) is used. Waveguides as those depicted in Fig. 2, consisting of two replica of the tapered laser under study are investigated.

A value of gain is assigned in the tapered gain sections together with proper fixed values for losses in the SA sections and outside the waveguide profile. A step index $\Delta n = 3\cdot10^{-3}$ is considered to guarantee that a single transverse mode is guided within the straight SA section. An iterative method is then applied. At first, the waveguide is excited with an initial field profile (e.g. Gaussian) and its evolution along the structure is computed. Proper normalisation of the field in z=3 mm allowing to include the effect of the output cavity loss at the SA side device facet (R_1) is considered. The field in z = 6 mm, is then normalized by the reflectivity at the gain facet (R_2) and reintroduced in z = 0; a new value for the gain in the tapered section is chosen and the propagation of the new field profile is again computed. This procedure is followed iteratively and the

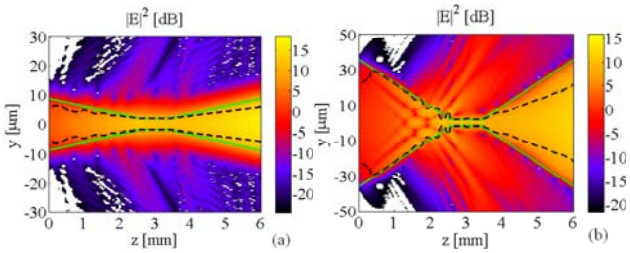

Figure 2 BPM simulation of the field profile evolution during forward (with z ranging from 3 mm to 6 mm) and backward (with z from 0 mm to 3 mm) propagation across the tapered device with θ = 0.3° (a) and θ = 1.5° (b). Black dashed lines represent a reduction of -3 dB with respect to the maximum field intensity in each longitudinal section of the device. Continuous green lines represent the waveguide profile, $y=\pm W(z)/2$, being $W(z)$ the ridge width as a function of the longitudinal coordinate z.

gain value is adjusted until a self-consistent field distribution is achieved. Optical intensity distributions $|E|^2(y,z)$ for the tapered devices with θ = 0.3° and θ = 1.5° are shown in Fig. 2a and Fig. 2b, respectively. For θ = 0.3°, the field transforms adiabatically along the tapered section, remaining well confined within the ridge; on the contrary for θ = 1.5°, radiation losses are clearly visible, reducing the overlap between the field profile and the SA transversal section.

From the calculated field distributions, values for Γ^k_{xy} and α_k^{int} are computed. Γ^k_{xy} is factorized in terms of the confinement factors along y and x directions: $\Gamma^k_{xy}= \Gamma_x \cdot \Gamma^k_y$. The confinement factor in the QD layers along the growth direction, Γ_x, is constant whereas Γ^k_y is calculated as:

$$\Gamma_y^k = \frac{1}{L_k} \int_{z\in L_k} \left\{ \frac{\int_{-W(z)/2}^{+W(z)/2} |E|^2(y,z)dy}{\int_{-\infty}^{+\infty} |E|^2(y,z)dy} \right\} dz \qquad (3)$$

The internal losses are then expressed as $\alpha_k^{int}= \alpha_0^{int}+ \Gamma_x(1- \Gamma^k_y)\ \alpha^{ext}$, being α^{ext} the absorption outside the ridge and α_0^{int} additional losses due to doping and defects. The obtained values for Γ^k_{xy}, α_k^{int} are shown together with W_k in Fig. 3 for the different tapered lasers.

4 Mode-locking simulation and discussion

Including the parameters obtained from the BPM simulations in the MS-DDE model, the ML regimes in the devices under study are then simulated. Fig. 4 shows maps of peak power and pulse width as a function of the applied gain current and SA reverse voltage for devices with θ = 0°, 0.3°, 0.6° whereas in Fig. 5 the same maps are reported for devices with θ = 1°, 1.5°. For small tapered full angles (θ = 0°, 0.3°), the maximum achievable average and peak power is limited by the onset of a large leading-edge (LE) instability in the pulse train with increasing current, furthermore the pulse duration remains always larger than 1 ps. With increasing θ, the LE instability tends to disappear even for current well above threshold whereas an instability at the trailing edge (TE) is found for moderate SA reverse voltages. Furthermore, at very large currents (large pulse energy), a pulse breakdown induced by the action of the large self-phase-modulation and dispersion is observed. With increasing θ, a significant pulse shortening is found so that for θ = 0.6°, 1°, ultra-short sub-picosecond pulses are achieved [1]. Such a reduction in the pulse width is attributed to the significant increase in the gain saturation energy in the gain section [1]. The shortest pulse width and largest peak power are achieved for θ = 1°. On the contrary increasing further the full angle (θ = 1.5°) no significant

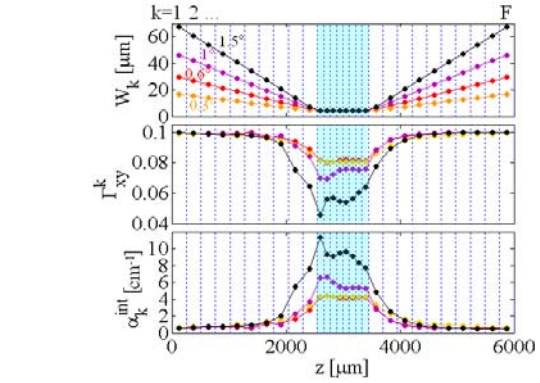

Figure 3 Ridge width W_k, field confinement factor Γ^k_{xy} and internal losses α_k^{int} for tapered devices with θ = 0.3°, 0.6°, 1°, 1.5°. Γ^k_{xy} and α_k^{int} have been extracted from BPM simulations.

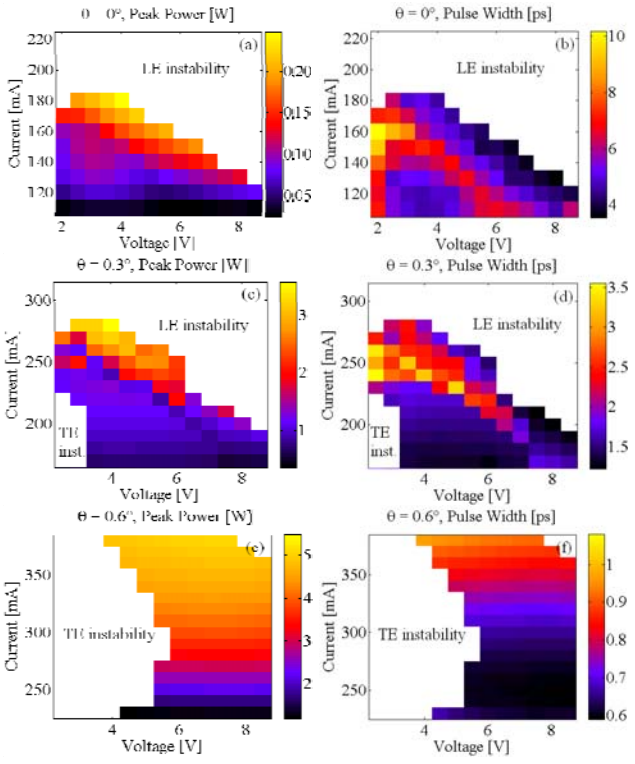

Figure 4 Maps of pulse peak power and pulse width as a function of the current applied to the gain section and voltage applied to the SA for devices with θ = 0°, 0.3°, 0.6°.

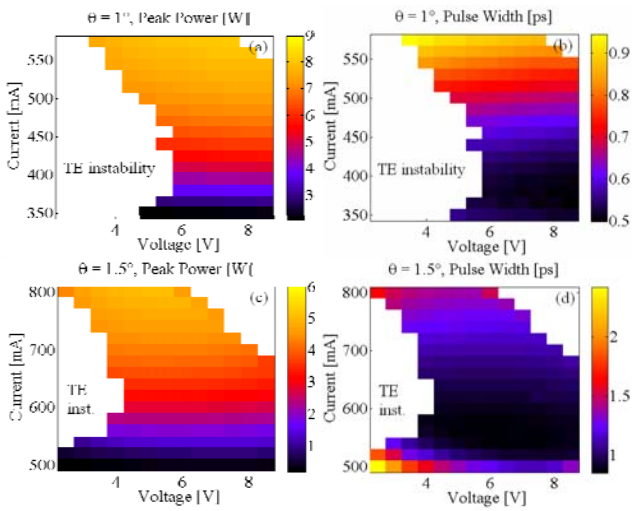

Figure 5 Maps of pulse peak power and pulse width as a function of the current applied to the gain section and voltage applied to the SA for devices with θ = 1°, 1.5°.

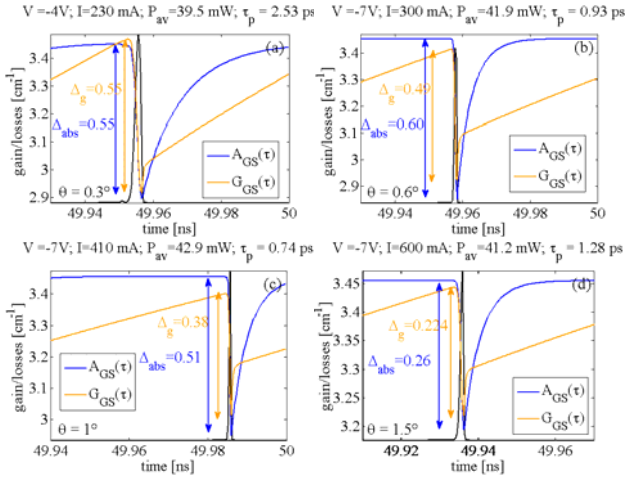

Figure 6 Net gain windows leading to different ML regimes: overall round trip losses $A_{GS}(\tau)$ and amplification $G_{GS}(\tau)$ are shown with the pulse envelope for θ = 0.3°, 0.6°, 1°, 1.5° and bias conditions leading to an average output power of about 40 mW.

improvements in the ML regimes are obtained. This is due to the fact that for too wide tapered full angles, the field profile does not transform adiabatically when travelling back across the tapered section and significant radiation of the field occurs (Fig. 2b); this leads to a large decrease in the overlap between the field profile and the reverse-biased SA (Fig. 3), reducing therefore the effectiveness of the SA in shaping the mode-locked pulses.

To further clarify the above discussion, the gain and absorption dynamics leading to the achieved mode-locked regime is investigated. The round trip gain $|R_{GS}(\tau)|$ is expressed as $|R_{GS}(\tau)|=\exp[(G_{GS}(\tau)-A_{GS}(\tau))\cdot(L_g^{Ring}+L_{SA}^{Ring})]$ where $G_{GS}(\tau)$ and $A_{GS}(\tau)$ are the overall amplification and losses experienced by the pulse within a single round trip [5]. In Fig. 6, $G_{GS}(\tau)$ and $A_{GS}(\tau)$ are shown together with the pulse envelope for mode-locked regimes achieved in the devices with θ = 0.3°, 0.6°, 1°, 1.5°. Bias conditions are chosen in such a way that stable mode-locked regimes characterized by almost the same average output power of 40 mW (i.e. by a comparable pulse energy) are achieved in all the devices. As expected, with increasing the tapered full angle, the maximum instantaneous saturation of $G_{GS}(\tau)$ significantly reduces (from Δ_g=0.55 cm^{-1} at θ=0.3° down to Δ_g=0.22 cm^{-1} at θ=1.5°) due to the increase in the gain saturation energy. On the contrary the maximum bleaching of the round trip losses $A_{GS}(\tau)$ (Δ_{abs}) slightly increases when θ is increased up to 0.6° but it starts to significantly decrease when θ is further increased up to 1.5°; this is directly related to the reduced overlap between the field profile and the reverse-biased SA section, limiting the maximum SA absorption bleaching and preventing further improvements in the achieved mode-locked regimes.

4 Conclusion

We proposed a computationally efficient approach for the simulation of tapered QD MLLs. We showed that increasing the taper full angle θ, a significant pulse shortening and enhanced peak power can be achieved. Optimum values for θ are found to be between 0.6° and 1°, for which an adiabatic transformation of the field profile along the tapered section is guaranteed and the generation of subpicosecond short pulses achieved. This approach was also applied to the design of gain guided tapered QD mode-locked lasers generating 15 W peak power and subpicosecond short pulses [2, 3].

Acknowledgements This work was funded by the European Community's 7th Framework Programme (FP7/2007–2013) under Grant Agreement 224338 (FAST-DOT project).

References

[1] M. G. Thompson, A. R. Rae, M. Xia, R. V. Penty, and I. H. White, IEEE J. Sel. Top. Quantum Electron. **15**(3), 661 (2009).
[2] D. I. Nikitichev et al., in: Proc. Conf. on Lasers and Electro-Optics Europe 2011, Munich, Germany (2011), CB3.4.
[3] L. Drzewietzki et al., in: Proc. Conf. on Lasers and Electro-Optics Europe 2011, Munich, Germany (2011), CB3.3.
[4] D. W. Reschner, E. Gehrig, and O. Hess, IEEE J. Quantum Electron. **45**(1), 21 (2009).
[5] M. Rossetti, P. Bardella, and I. Montrosset, IEEE J. Quantum Electron. **47**, 569 (2011).
[6] A. G. Vladimirov and D. Turaev, Phys. Rev. A **72**(3), 033808-1 (2005).
[7] A. G. Vladimirov, U. Bandelow, G. Fiol, D. Arsenijević, M. Kleinert, D. Bimberg, A. Pimenov, and D. Rachinskii, J. Opt. Soc. Am. B **27**, 2102 (2010).
[8] M. Gioannini and I. Montrosset, IEEE J. Quantum Electron. **43**(10), 941 (2007).
[9] M. Rossetti, P. Bardella, and I. Montrosset, IEEE J. Quantum Electron. **47**, 139 (2011).
[10] K. Okamoto, Fundamental of Optical Waveguides (Academic Press, 2000).